Electronic Supplementary Material (ESI) for Environmental Science: Nano.

The synergistic photocatalytic effects of surface-modified g-C_3N_4 in simple and complex pollution systems based on the macro-thermodynamics model

Kexin Li[a,b], Dongxiao Zhao[a,b], Yawen Li[a,b], Shenglian Luo[a,b,*] and Zhentao Zhou[a,b]

[a]*Key Laboratory of Jiangxi Province for Persistent Pollutants Control and Resources Recycle, NanChang Hangkong University, NanChang 330063, People's Republic of China*

[b]*National-Local Joint Engineering Research Center of Heavy Metals Polluants Control and Resource utilization, NanChang Hangkong University, NanChang 330063, People's Republic of China*

**Corresponding author:*
E-mail address: sllou@hnu.edu.cn

Table S1 The atomic concentrations of C, N, O, and Cl elements in the BCQDs, g-C_3N_4, H^+/g-C_3N_4, BCQDs/g-C_3N_4, and H^+/BCQDs/g-C_3N_4.

Photocatalysts	C	N	O	Cl
BCQDs	74.36	0.97	24.67	–
g-C_3N_4	54.50	42.13	3.37	–
H^+/g-C_3N_4	57.70	35.62	6.30	0.38
BCQDs/g-C_3N_4	52.89	43.40	3.71	–
H^+/BCQDs/g-C_3N_4	53.42	41.59	4.63	0.36

Table S2 The Cr(VI) reduction kinetic parameters of as-prepared g-C_3N_4, H^+/g-C_3N_4, BCQDs/g-C_3N_4, and H^+/BCQDs/g-C_3N_4.

Photocatalysts	First order kinetic plot	K (min^{-1})	R^2
g-C_3N_4	–0.0000t–0.0088	0.0000	0.1381
H^+/g-C_3N_4	–0.0053t+0.2843	0.0053	0.9768
BCQDs/g-C_3N_4	–0.0033t–0.0695	0.0033	0.9923
H^+/BCQDs/g-C_3N_4	–0.1043t+5.9681	0.1043	0.9554

Table S3 The atomic concentrations of C, N, O, and Cl elements in the H^+/BCQDs/g-C_3N_4 before and after photocatalytic reduction of aqueous Cr(VI).

Photocatalysts	C	N	O	Cl
H^+/BCQDs/g-C_3N_4 (before)	53.42	41.59	4.63	0.36
H^+/BCQDs/g-C_3N_4 (after)	40.29	56.12	3.56	0.04

Table S4 The 4-FP degradation kinetic parameters of as-prepared g-C_3N_4, H^+/g-C_3N_4, BCQDs/g-C_3N_4, and H^+/BCQDs/g-C_3N_4.

Photocatalysts	First order kinetic plot	K (min^{-1})	R^2
g-C_3N_4	–0.0116t+0.6501	0.0116	0.9877
H^+/g-C_3N_4	–0.0512t+3.2674	0.0512	0.9156
BCQDs/g-C_3N_4	–0.0072t+0.4099	0.0072	0.9473
H^+/BCQDs/g-C_3N_4	–0.0145t+0.7816	0.0145	0.9913

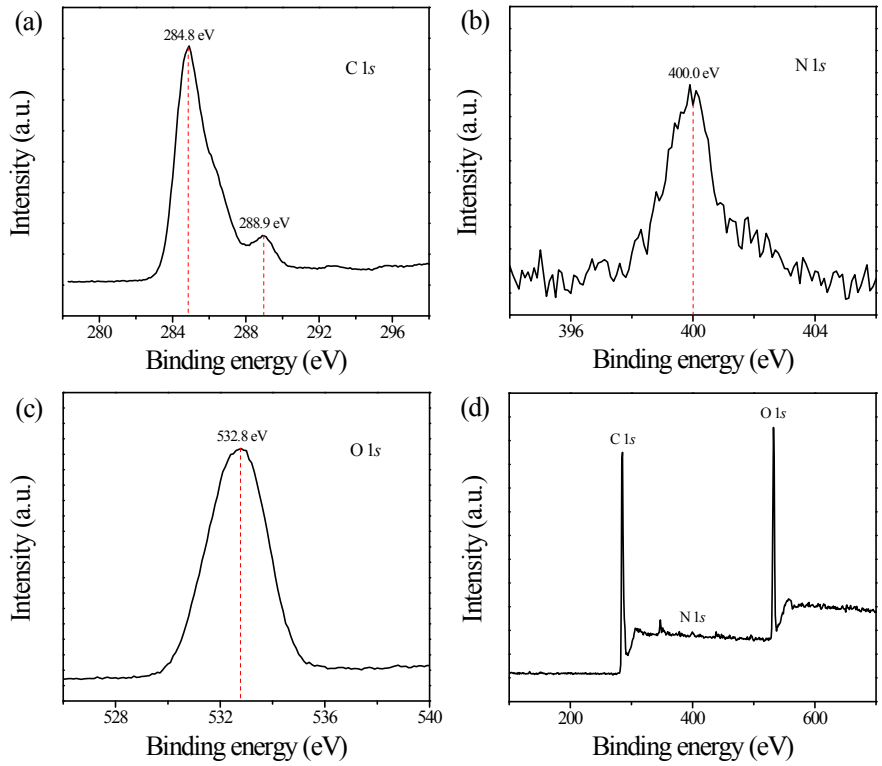

Fig. S1 High-resolution (a, b, and c) and full-range (d) XPS of as-prepared BCQDs in the C 1*s*, N 1*s*, and O 1*s* binding energy regions.

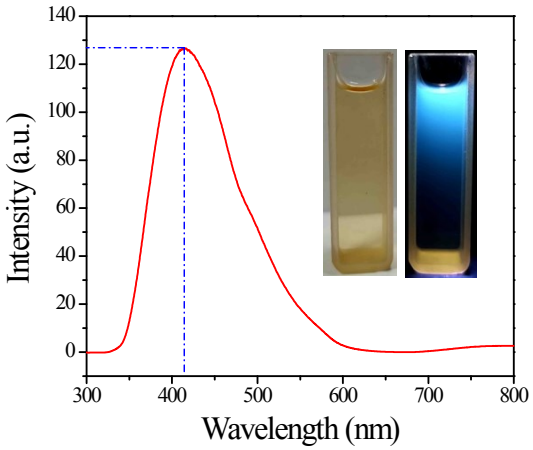

Fig. S2 PL spectrum and corresponding fluorescence image of as-prepared BCQDs aqueous precursor.

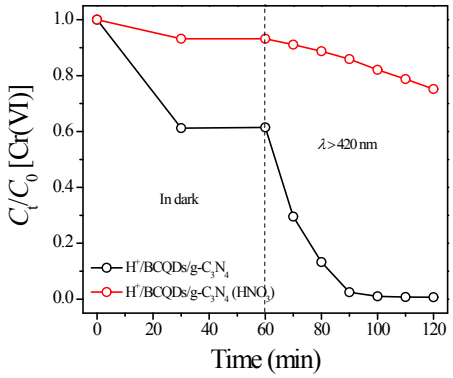

Fig. S3 The photocatalytic activity comparison of H^+/BCQDs/g-C_3N_4 and HNO_3 treated H^+/BCQDs/g-C_3N_4 toward aqueous Cr(VI) reduction.

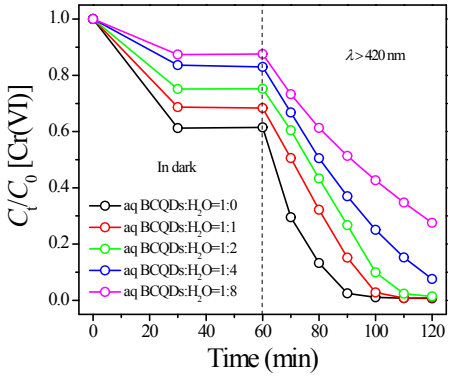

Fig. S4 Influence of BCQDs aqueous precursor concentrations on the photocatalytic activities of H^+/BCQDs/g-C_3N_4 toward aqueous Cr(VI) reduction.

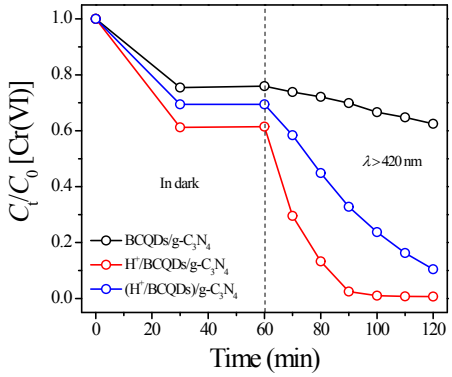

Fig. S5 The photocatalytic activity comparison of BCQDs/g-C_3N_4, H^+/BCQDs/g-C_3N_4, and (H^+/BCQDs)/g-C_3N_4 toward aqueous Cr(VI) reduction.

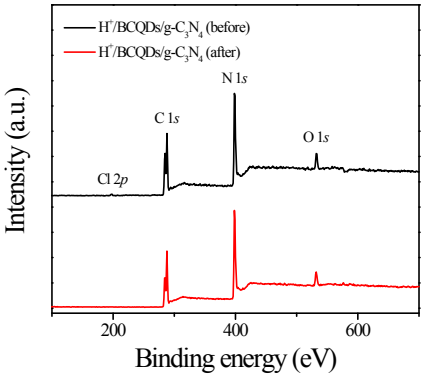

Fig. S6 Full-range XPS of H^+/BCQDs/g-C_3N_4 in the C 1*s*, N 1*s*, O 1*s*, and Cl 2*p* binding energy regions before and after photocatalytic reduction of aqueous Cr(VI).

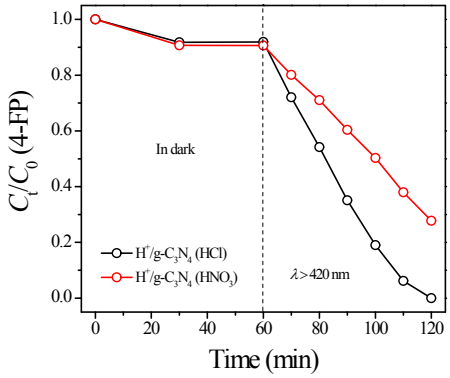

Fig. S7 Photocatalytic degradation of aqueous 4-FP by using HCl or HNO_3 treated g-C_3N_4.

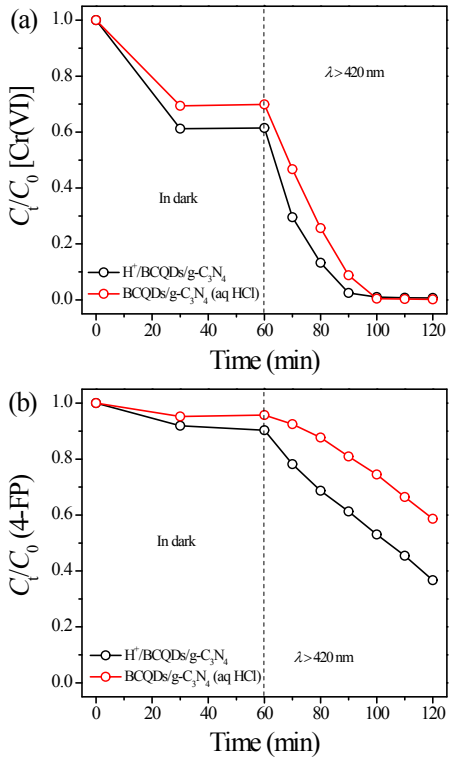

Fig. S8 The photocatalytic activity comparison of H+/BCQDs/g-C_3N_4 and BCQDs/g-C_3N_4 (aq HCl) toward aqueous Cr(VI) reduction (a) and 4-FP degradation (b).